

Article

Not peer-reviewed version

Cytokine Receptor Like Factor 1 (CRLF1) and its Role in Osteochondral Repair

[Fenglin Zhang](#) , Andrew J. Clair , John F. Dankert , You Jin Lee , Kirk A. Campbell , [Thorsten Kirsch](#) *

Posted Date: 19 March 2024

doi: 10.20944/preprints202403.1072.v1

Keywords: osteochondral defect repair; CRLF1; Mesenchymal stem cells; chondrogenic differentiation; chondrocytes



Preprints.org is a free multidiscipline platform providing preprint service that is dedicated to making early versions of research outputs permanently available and citable. Preprints posted at Preprints.org appear in Web of Science, Crossref, Google Scholar, Scilit, Europe PMC.

Copyright: This is an open access article distributed under the Creative Commons Attribution License which permits unrestricted use, distribution, and reproduction in any medium, provided the original work is properly cited.

Article

Cytokine Receptor Like Factor 1 (CRLF1) and Its Role in Osteochondral Repair

Fenglin Zhang ¹, Andrew J. Clair ², John F. Dankert ³, You Jin Lee ³, Kirk A. Campbell ³ and Thorsten Kirsch ^{3,4,*}

¹ Department of Urology, New York University Grossman School of Medicine, New York, NY, USA; fenglin.zhang@nyulangone.org

² Rothman Orthopedic Institute, Orlando, FL, USA; Andrew.Clair@Rothmanortho.com

³ Department of Orthopedic Surgery, New York University Grossman School of Medicine, New York, NY, USA; john.dankert@nyulangone.org (J.F.D.); kirk.campbell@nyulangone.org (K.A.C.); thorsten.kirsch@nyulangone.org (T.K.)

⁴ Department of Biomedical Engineering, New York University Tandon School of Engineering, New York, NY, USA; Thorsten.kirsch@nyulangone.org

* Correspondence: Thorsten.kirsch@nyulangone.org; Tel.: ++1-646-754-1834

Abstract: Background: Since cytokine receptor like factor 1 (CRLF1) has been implicated in tissue regeneration, we hypothesized that CRLF1 released by mesenchymal stem cells can promote the repair of osteochondral defects. Methods: The degree of a femoral osteochondral defect repair in rabbits after intra-articular injections of bone marrow derived mesenchymal stem cells (BMSCs) that were transduced with empty adeno associated virus (AAV) or AAV containing CRLF1 was determined by morphological, histological and microCT analyses. The effects of CRLF1 on chondrogenic differentiation of BMSCs or catabolic events of interleukin-1beta-treated chondrocyte cell line TC28a2 were determined by alcian blue staining, gene expression levels of cartilage and catabolic marker genes using real time PCR analysis, and immunoblot analysis of Smad2/3 and STAT3 signaling. Results: Intra-articular injections of BMSCs overexpressing CRLF1 markedly improved repair of a rabbit femoral osteochondral defect. Overexpression of CRLF1 in BMSCs resulted in the release of a homodimeric CRLF1 complex that stimulated chondrogenic differentiation of BMSCs via enhancing Smad2/3 signaling, whereas the suppression of CRLF1 expression inhibited chondrogenic differentiation. In addition, CRLF1 inhibited catabolic events in TC28a2 cells cultured in an inflammatory environment, while a heterodimeric complex of CRLF1 and Cardiotrophin like Cytokine (CLC) stimulated catabolic events via STAT3 activation. Conclusion: A homodimeric CRLF1 complex released by BMSCs enhanced the repair of osteochondral defects via the inhibition of catabolic events in chondrocytes and the stimulation of chondrogenic differentiation of precursor cells.

Keywords: osteochondral defect repair; CRLF1; Mesenchymal stem cells; chondrogenic differentiation; chondrocytes

1. Introduction

Cartilage injuries of the knee affect approximately 900,000 Americans annually, resulting in more than 200,000 surgical procedures [1]. These injuries are frequently associated with pain, diminished joint functionality, and reduced life quality. Various surgical techniques to repair or regenerate cartilage injuries are used, including microfracture, cell-based restorative techniques, and osteochondral allografts and autografts [2]. Despite the advancement of these surgical techniques, full-thickness chondral or osteochondral defects still remain a major challenge, because none of the surgical methods, including the cell-based approaches, form native hyaline cartilage. As a consequence, the poor quality of regenerated cartilage in the defect site leads to the early onset of post-traumatic osteoarthritis (PTOA) requiring eventual joint replacement at relatively young age. There is an urgent need for new ways to repair cartilage defects or lesions to prevent or delay the onset of early PTOA.

Cytokine receptor-like factor 1 (CRLF1) belongs to the IL-6 superfamily or the gp130 cytokine family [3,4]. CRLF1, as well as the other IL-6 cytokines, can drive both regenerative and degenerative outcomes via selective and context/cell specific activation of various signaling modules within gp130 receptor [3–5]. CRLF1 is expressed in bone and cartilage, and several studies have shown increased expression of CRLF1 in early-stage OA cartilage [3,6–8]. Human mutations in CRLF1 are associated with Crisoni/cold sweating syndromes and lead to early neonatal death in mice due to a suckling defect [3]. CRLF1 can form a heterodimeric complex with another member of the IL-6 superfamily, cardiotrophin-like cytokine (CLC) [3,4]. CRLF1/CLC complex signaling involves the use of a receptor subunit ciliary neurotrophic factor receptor (CNTFR). The resulting complex then recruits the ubiquitously expressed receptor subunit gp130 and LIFR [3,4]. In addition, CRLF1 can also form a homodimeric complex that signals in the absence of CLC [3,9]. More importantly, the homodimeric CRLF1 complex results in different signaling and cellular responses than the CRLF1/CLC heterodimeric complex [3,9]. Previous studies have suggested that the heterodimeric CRLF1/CLC complex signaling often leads to degenerative processes, while homodimeric CRLF1 complex signaling leads to tissue protection and regeneration [3,9]. For example, a previous study revealed that the CRLF1 homodimer shows neuro-protective effects suggesting that CRLF1 may be exploited for therapeutic advantage in adults with neurodegenerative conditions [3,9].

Little, however, is known about the function of CRLF1 in articular cartilage and in cartilage repair. Previous studies have shown that CRLF1 is highly upregulated in osteoarthritic and damaged cartilage suggesting a role of CRLF1 in osteoarthritis [4,6–8]. In addition, it was shown that CRLF1/CLC complex stimulated proliferation of the chondrogenic cell line ATDC5 while inhibiting the expression of two cartilage marker proteins, type II collagen and aggrecan [6]. In this study, we analyzed how CRLF1 affects chondrogenic differentiation of bone marrow-derived mesenchymal stem cells (BMSCs), catabolic events of articular chondrocytes in an inflammatory environment and ultimately repair of an osteochondral defect in rabbits. Our findings show that intra-articular injections of BMSCs overexpressing CRLF1 markedly improved the repair of osteochondral defects

2. Materials and Methods

2.1. Reagents and Solutions

Orthovisc® high molecular weight hyaluronan (HMWHA, 1-3 million Daltons) was obtained from DePuy Synthes (Johnson & Johnson, Raynham, MA). Orthovisc® HMWHA is an FDA-approved product for the treatment of osteoarthritis.

2.2. Cell Culture

Human BMSCs were obtained from RoosterBio, Inc. (Frederick, MD, USA). All cells for experiments were maintained for up to two passages. These human BMSCs are well characterized and are able to differentiate into osteoblasts, chondrocytes and adipocytes. For this study, BMSCs from female and male donors were used. Human BMSCs were expanded and cultured in RoosterNourish™-MSC medium according to the manufacturer's instructions. One day before transduction, cells were plated in appropriate seeding density so that cells were 30-50% confluent at the time of transduction. On the day of transduction, $\sim 1 \times 10^6$ BMSCs in 3ml medium were cultured in the presence of 2.0×10^{13} genome copies (GC)/ml of adeno-associated virus (AAV). Cells were incubated at 37°C in a humidified 5% CO₂ incubator overnight. Then, medium was replaced with fresh medium and cultured until harvesting or analysis. The expression levels of CRLF1 were determined by analyzing the mRNA levels of CRLF1 using real time PCR analysis. The amount of CRLF1 in the culture medium was analyzed by SDS gel electrophoresis and immunoblotting with antibodies specific for CRLF1. The presence of the homodimeric form of CRLF1 was determined by gel electrophoresis under non-reducing conditions and immunoblotting with antibodies specific for CRLF1 and CLC.

The human chondrocyte cell line TC28a2 was obtained from Millipore and cultured according the manufacturer's instructions. Once TC28a2 cells reached confluency, they were switched to serum-

free medium for 24 h followed by treatment with 10ng/ml human interleukin-1beta (IL-1b; R&D Systems, Minneapolis, MN) for 24h in the absence or presence of recombinant human CRLF1/CLC complex (100µM; R&D Systems). To determine how CRLF1 affects IL-1b-treated TC28a2 cells, we transfected TC28a2 cells with the expression vector pcDNA containing CRLF1 as described by us previously [10]. 72 h after transfection, cells were treated with 10ng/ml IL-1b for 24h in serum-free conditions.

2.3. Pellet Formation and Chondrogenic Induction

Human BMSC transduced with empty AAV or CRLF1-AAV cultures were trypsinized and 4×10^5 cells were centrifuged at $500 \times g$ for 10 min. Cells were left in pellet form in the tubes overnight and became aggregated. The culture medium was replaced with chondrogenic medium consisting of Dulbecco's Modified Eagle's Medium, High Glucose (4.5g/l; #11995-065, Gibco) containing ITS+ Premix (6.25 µg/ml each of insulin, transferrin, and selenous acid; 1.25 mg/ml bovine serum albumin; and 5.35 µg/ml linoleic acid; Corning, Corning, NY, USA), 50 µg/ml L-ascorbic acid-2-phosphate (Sigma), 0.1 µM dexamethasone (Sigma), and 10 ng/ml transforming growth factor-beta1 (TGF-β1; Peprotech, Rocky Hill, NJ). For siRNA experiments, cells were transfected with control siRNA or CRLF1-specific siRNA using the siPORT NeoFX reagent from Ambion. After transfection, cells were cultured for up to 14 days in differentiation medium in pellets. The medium was changed every other day. Total RNA was analyzed 14 days of pellet cultures. In addition, alcian blue (Sigma-Aldrich) in 3% glacial acetic acid solution of sections of the pellets was performed to determine the degree of chondrogenic differentiation.

2.4. Adeno-Associated Virus (AAV) Containing Full Length CRLF1

The AAV vector was generated after cloning full length human CRLF1 into adeno-associated vector pENN.AAV.CB&Cl.eGFP.WPRErBG (Plasmid# 105542; Addgene, Watertown, MA). Large scale AAV1 packaging and purification (titer $> 1 \times 10^{13}$ GC/ml) was performed by Vigene Biosciences, Inc. (Rockville, MD).

2.5. Reverse Transcription–Polymerase Chain Reaction (PCR) and Real-Time PCR Analysis

Total RNA was isolated from BMSC or TC28a2 cell cultures using a RNeasy Mini kit (Qiagen, Valencia, CA). Levels of messenger RNA (mRNA) of aggrecan, CLC, CRLF1, interleukin-6 (IL-6), matrix metalloproteinase-13 (MMP-13), Sox-9, type II collagen (α1(II)), type X collagen (α1(X)) were quantified by real-time PCR as previously described [11]. Briefly, 1 µg of total RNA was reverse transcribed using the High Capacity cDNA synthesis kit (Applied Biosystems, Foster City, CA). A 1:100 dilution of the resulting cDNA was used as the template to quantify the relative content of mRNA by real-time PCR (ABI StepOne Plus; Applied Biosystems) using the appropriate primers and RT² SYBR Green ROX FAST Mastermix (Qiagen). PCRs were performed at 95°C for 10 minutes, followed by 40 cycles of 95°C for 10 seconds and 60°C for 30 sec, and 1 cycle of 95°C for 15 seconds and 60°C for 1 minute. The housekeeping 18S and RPL13a RNA were amplified at the same time and used as an internal control. The cycle threshold values for 18S and RPL13a RNA and the samples were measured and calculated. Relative transcript levels were calculated as $x = 2^{-\Delta\Delta C_t}$, in which $\Delta\Delta C_t = DE - DC$, $DE = C_{t_{exp}} - C_{t_{(18S+RPL13a)}}$, and $DC = C_{t_{ctrl}} - C_{t_{18S}}$.

2.6. Sodium Dodecyl Sulfate (SDS)-Polyacrylamide Gel Electrophoresis and Immunoblotting

Medium was collected from cultured BMSCs transduced with empty AAV or AAV containing CRLF1. After concentrating the medium, aliquots of the medium were combined with $4 \times$ NuPAGE SDS sample buffer without and with reducing agent (Invitrogen), denatured at 70 °C for 10 min, and analyzed by electrophoresis in 10% bis-Tris polyacrylamide gels. Samples were electroblotted onto nitrocellulose filters after electrophoresis. After blocking with a solution of low-fat milk protein, blotted proteins were immunostained with primary antibodies specific for b-actin. CRLF1 (ab211438, Abcam, Boston, MA) or CLC (ab154798, Abcam), total STAT3 (#9139, Cell Signaling Technology,

Danvers, MA), phosphorylated STAT3 (#9145, Cell Signaling Technology), total Smad2 and 3, phosphorylated Smad 2, and phosphorylated Smad3 (SMAD2/3 Antibody Sampler Kit #12747, Cell Signaling Technology, Danvers, MA), and then peroxidase-conjugated secondary antibody (Pierce). The signal was detected by enhanced chemiluminescence (Pierce) as previously described.[11]

2.7. Femoral Osteochondral Defect Model

This study utilized a validated rabbit femoral osteochondral defect model, whereby male New Zealand white rabbits (weighing 2.5-3 kg) were used to construct osteochondral defect models using a previously described protocol [12–14]. Rabbits were allowed to acclimatized for 7 days before cartilage defect surgery. After anesthesia, a stainless-steel drill was used to create 4-mm diameter and 4-mm deep cylindrical defects in the center of the distal articular cartilage of the femur. Surgery was performed on skeletally mature New Zealand White (NZW) rabbits (6 – 7-month-old females, average weight 3.9 kg) according to our Institutional Animal Care and Use Committee (IACUC)–approved protocol. After cartilage defect surgery, rabbits were randomly divided into the three treatment groups, with each group having the same number of rabbits (n = 5 per group). Group 1 received three intra-articular injections of 1mg/ml high molecular weight hyaluronan (HMWHA, 12mg/ml) in phosphate-buffered saline (PBS); Group 2 received three intra-articular injections of 1×10^6 BMSCs transduced with empty AAV in HMWHA/PBS; Group 3 received three intra-articular injections of 1×10^6 BMSCs transduced with AAV-CRLF1 in HMWHA/PBS. Each rabbit received three intra-articular injections. The first intra-articular injection was performed directly after osteochondral defect surgery followed by the second injection one week after surgery and the third intra-articular injection two weeks after surgery. The number of animals per group was calculated based on the statistical power for detecting > 25% difference in the average macroscopic and histological scores caused by intra-articular injections of BMSCs transduced with empty AAV in HMWHA/PBS compared to intra-articular injections of HMWHA/PBS alone. Postoperatively, the animals were permitted to move freely within their cages.

2.8. Macroscopic Evaluation

After 12 weeks, rabbits were euthanized according to IACUC protocol and knees were harvested from each animal. The degree of articular cartilage repair was assessed by two blinded and independent graders for each knee using the International Cartilage Repair Society (ICRS) macroscopic evaluation system [15]. This score specifically assesses 3 features of articular cartilage repair: the degree of defect repair, integration to border zone, and macroscopic appearance. Each feature was scored from 0 to 4, for a maximum possible score of 12.

2.9. MicroCT Examination

After washing with PBS, rabbit femurs were incubated in PBS containing the ionic contrast agent Hexabrix (40% v/v, Mallinckrodt, Hazelwood, MO) for 6 h. All joints were evaluated in a scanning tube providing a voxel size of 10.5 mm and scanned at 55 kV, 181 mA, 110 min of acquisition time using a Skyscan 1172 (Bruker, Billerica, MA). During scanning the samples were wrapped in paper soaked in PBS to avoid dehydration. MicroCT analysis of bone and cartilage volume was performed using CTvox software to reconstruct 2D and 3D images. Amira software (FEI, Oregon-USA) was used to reconstruct femur joints from microCT data based on differential density of bone and Hexabrix-treated cartilage.

2.10. Histological and Immunohistochemical Defect Repair Scoring

After gross examination, the distal parts of the femur were removed, trimmed and placed in 4% formalin followed by 15% ethylenediaminetetraacetic acid (EDTA) w/v in PBS decalcification solutions. The decalcified specimens were embedded in paraffin and cut to 5 μ m sections. Histological evaluation was made on a series of sections cut through the centers of the repairs/defects. The sections were stained with safranin O. For immuno-histochemical staining, the sections were

deparaffinized and rehydrated followed by treatment with 3% v/v hydrogen peroxide to block endogenous peroxidase activity. For immunostaining for type I and type II collagen staining, sections were pre-treated with Proteinase K solution at 37°C for 15 min. The sections were subsequently incubated with 10% horse serum in PBS v/v at room temperature for 30 min, to reduce non-specific staining before overnight incubation with mouse anti-type I collagen monoclonal antibody (Abcam, ab6308) at a 1:200 dilution, mouse anti-type II collagen monoclonal antibody (Invitrogen, 2B1.5. MA1-37493) at 1:200 dilution in PBS containing 0.1% w/v BSA at 4°C. The sections were then incubated with biotinylated universal immunoglobulin secondary antibody (Vectastain Elite ABC System) at 1:500 dilution for 30 min at room temperature. Finally, the sections were incubated with 20 mg diaminobenzidine and 5 ml hydrogen peroxide (30%) in 100 ml PBS for 5 min at room temperature. Sections incubated with PBS without primary antibodies were used as a negative control. The sections were evaluated microscopically and morphological features of the repaired cartilage tissue were evaluated using a grading scale adopted from the International Cartilage Repair Society (ICRS) visual histological assessment scale, consisting of six categories with a total score ranging from 0 to 13 points [16]. In addition, we semi-quantitatively scored the intensity of immunostaining for type I and type II collagen using a grading scale consisting of 4 categories (abundant, moderate, slight and no staining) with a total score ranging from 0 to 3. Both scores were combined resulting in a total score from 0 to 19 (Supplementary Table S1). The histological and immuno-histological degrees of cartilage repair were assessed by two blinded reviewers. For each knee joint five sections spaced 50µm apart were scored. Data are expressed as total summed average score from the two reviewers.

2.11. Statistical Analysis

Data are expressed as means \pm 95% Confidence Interval. To test differences in group mean, we used analysis of variance (ANOVA). After we confirmed that the groups differ in their outcomes, we performed Tukey's post hoc test to identify groups with better outcomes. Statistical analyses were performed using GraphPad Prism, version 9.0. In all groups, *p*-values < 0.05 indicated statistical significance.

3. Results

3.1. BMSCs Overexpressing CRLF1 Improve Osteochondral Repair

We utilized a validated rabbit osteochondral defect model [12–14]. After the surgical generation of the osteochondral defect, rabbits received three intra-articular injections of HMWHA in PBS, BMSCs transduced with empty AAV (BMSC) resuspended in HMWHA/PBS, or BMSCs transduced with AAV containing *CRLF1* (BMSC-CRLF1) immediately after surgery and 1 and 2 weeks after surgery. Rabbits were euthanized at 12 weeks post-surgery. The degree of repair was analyzed by morphological and histological analyses using validated scoring systems [15,16].

Gross Observations – At week 12 postoperatively, cartilage-like repair tissue that had integrated with the original tissue has filled the osteochondral defect in the rabbit knee joints injected with BMSCs transduced with AAV-CRLF1 mixed in HMWHA/PBS (BMSC-CRLF1), while small clefts and fissures were observed in knee joints injected with BMSCs transduced with empty AAV mixed in HMWHA/PBS (BMSC). The macroscopic appearance of the repair cartilage of BMSC-CRLF1-injected knee joints was mostly smooth with some minor fibrillations, while the macroscopic appearance of the repair cartilage of BMSC-injected knee joints was more fibrillated with areas showing small cracks and scattered fissures. The repair cartilage of HMWHA-injected knee joints showed more areas with cracks and scattered fissures than BMSC-injected knee joints (Figure 1A). The overall mean score on week 12 suggested grade II or nearly normal healing (score 11-8) of cartilage defects in BMSC-CRLF1-injected knee joints, between grade III (score 11-8) and grade II (score 7-4) healing of cartilage defects in BMSC-injected knee joints, and mostly grade III or abnormal healing (score 7-4) of cartilage defects in HMWHA-injected knee joints (Figure 1B).

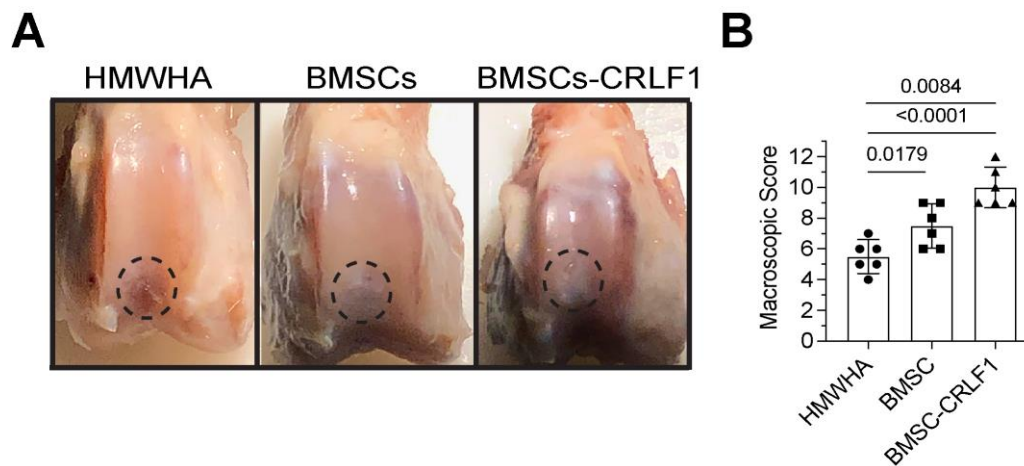


Figure 1. Gross appearance of osteochondral defect repair in rabbit knee joints. **A:** Gross appearance at 12 weeks post-surgery showing repair of osteochondral defects in a rabbit model after intra-articular injections of HMWHA (12mg/ml in PBS), BMSCs transduced with empty AAV (BMSCs-AAV) in HMWHA/PBS, or BMSCs transduced with AAV containing CRLF1 (BMSCs-CRLF1). Dotted circle indicates repair site. **B:** ICRS macroscopic osteochondral repair assessment for three intra-articular HMWHA injections, BMSCs-AAV injections, or BMSCs-CRLF1 injections (n = 6 knees per group). Values are mean \pm SD. Statistical analysis between the two groups was carried out using Tukey's post hoc test; p values are indicated above the graphs.

Histological Analysis – Histological analysis of five sections 50 μ m apart of the repair site 12 weeks post-surgery revealed that the defect site of knee joints injected with BMSC-CRLF1 was filled with hyaline cartilage that was nicely stained with safranin O, while the reparative tissue in femurs of rabbits injected with BMSC showed a more fibrotic appearance with less intense safranin O staining. The reparative tissue in femurs of rabbits injected with HMWHA showed mostly fibrotic tissue. The repair tissue of cartilage defects in femurs of rabbits injected with BMSC-CRLF1 showed a better integration with the original tissue, while BMSC injected knee joints showed a more obvious cleft and defect. While BMSC-CRLF1 injected knee joints showed well-formed new subchondral bone in the defect, BMSC-injected and HMWHA-injected knee joints showed mostly cartilaginous and fibrous tissue in the subchondral defect. (Figure 2A).

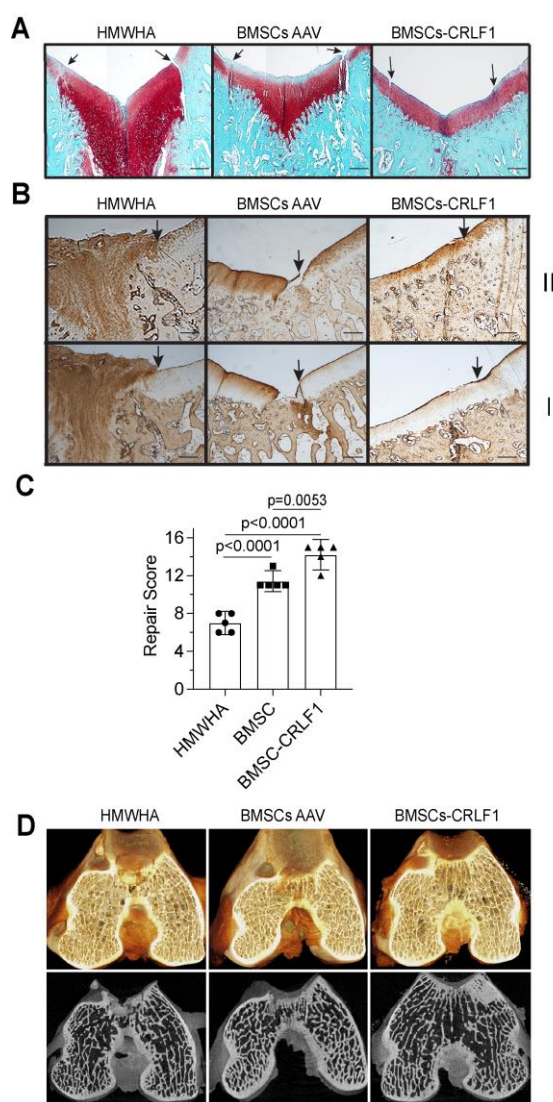


Figure 2. Histological and micro-CT assessment of the repair of osteochondral defects in rabbit knee joints. Histological and micro-CT assessment of osteochondral defect repair after three intra-articular injections of HMWHA/PBS, BMSCs transduced with empty AAV in HMWHA/PBS (BMSCsAAV), or BMSCs transduced with AAV containing *CRLF1* (BMSCs-CRLF1) in HMWHA/PBS ($n=5$ per group) at 12 weeks. **A:** Safranin O red staining images of osteochondral repair after HMWHA/PBS, BMSCsAAV, BMSCsAAV-CRLF1 intra-articular injections. Arrows indicate the repair site. Bar, 200 μ m. **B:** Images of sections from osteochondral repair sites after intra-articular injections of HMWHA/PBS, BMSCsAAV, or BMSCsAAV-CRLF1 immunostained with antibodies specific for type II collagen (II) or type I collagen (I). Arrows indicate the border of the repair site. Bar, 200 μ m. **C:** Histological evaluation of osteochondral repair after intra-articular injections of HMWHA/PBS, BMSCsAAV or BMSCsAAV-CRLF1 using the ICRS Visual Histological Assessment Scale as described in Suppl. Table S1 ($n = 5$ per group). Values are expressed as mean \pm SD. Statistical analysis between the two groups was carried out using Tukey's post hoc test. p values are indicated above the graphs. **D:** Images of three-dimensional micro-CT reconstructions of hexabrix-stained osteochondral repair tissue in the HMWHA/PBS-injected, BMSCsAAV-injected, or BMSCsAAV-CRLF1-injected groups.

Immunohistochemical staining for type I and type II collagen revealed that the repair cartilage tissue of BMSC-CRLF1-injected knee joints only showed immunostaining for type II collagen but not for type I collagen indicative for hyaline cartilage, whereas the repair tissue of BMSC-injected knee joints showed immunostaining for type I and type II collagen indicative of fibro-cartilage (Figure 2B). HMWHA-injected knee joints showed intense immunostaining of type I and type II collagen in the entire repair tissue (Figure 2B). Consequently, the repair score was significantly higher in BMSC-

CRLF1-injected knee joints than BMSC-injected knee joints. HMWHA-injected knee joints had the lowest repair score (Figure 2C).

MicroCT reconstruction images of hexabrix-stained knee joints showed the most improved subchondral bone regeneration in knee joints injected with BMSC-CRLF1 at 12 weeks compared to knee joints injected with BMSC- or HMWHA-injected knee joints. More neo-bone formed in the knee joints injected with BMSC-CRLF1 than in the knee joints injected with BMSC. The fewest neo-bone was found in knee joints injected with HMWHA (Figure 2D).

3.2. Effect of CRLF1 on Chondrogenesis

Human BMSCs, when cultured in a pellet culture system in chondrogenic differentiation medium underwent chondrogenic differentiation as indicated by increased glycosaminoglycan productions as determined by alcian blue staining of histological sections of these pellets. Reducing CRLF1 expression using siRNA in BMSC pellet cultures in chondrogenic medium resulted in a markedly decreased alcian blue staining compared to pellets that were transfected with control siRNA (Figure 3A). In contrast, pellets of BMSCs overexpressing CRLF1 after transduction with AAV containing *CRLF1* showed markedly enhanced alcian blue staining compared to the pellet of BMSCs transduced with empty AAV revealing an increased rate of chondrogenic differentiation (Figure 3A). Chondrogenic differentiation of human BMSCs in pellet cultures was performed in the presence of TGF- β 1. TGF- β 1 activated Smad2 and Smad3 signaling as revealed by immuno-positive bands of the phosphorylated forms of Smad2 and Smad3 on immunoblots of lysates from BMSCs (Figure 3B). More intense immuno-positive bands for Smad2 and Smad3 were present on the immunoblot of lysates from BMSCs transduced with AAV-*CRLF1* compared to lysates from BMSCs transduced with empty AAV (Figure 3B).

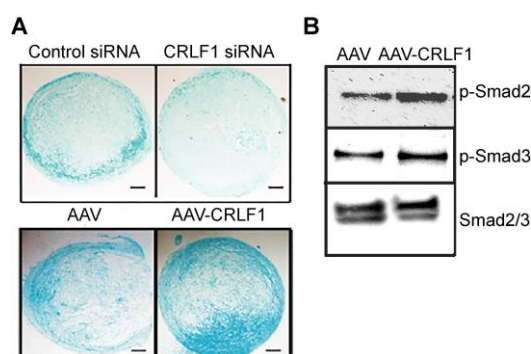


Figure 3. Chondrogenic differentiation of human BMSCs overexpressing CRLF1 **A:** Alcian blue staining of sections of BMSC pellets transfected with control siRNA (Control siRNA) or siRNA specific for CRLF1 (CRLF1 siRNA) after 6 days in chondrogenic differentiation medium; sections of BMSC pellet transduced with empty AAV (AAV) or transduced with AAV containing CRLF1 (AAV-CRLF1) after 6 days in chondrogenic differentiation medium. Bar, 100 μ m. **B:** Phosphorylated (p-Smad) and total Smad2 and Smad3 immunoblots of lysates from BMSCs transduced with empty AAV (AAV) or from BMSCs transduced with AAV-CRLF1. Cells were treated for 60min with TGF β 1.

Type II collagen, aggrecan, and Sox-9 mRNA levels were markedly higher in BMSC pellets transduced with AAV-*CRLF1* than in BMSC pellets transduced with empty AAV when cultured for 8 days in chondrogenic differentiation medium, whereas hypertrophic marker (MMP-13, type X collagen) mRNA levels were decreased in BMSC pellets transduced with AAV-*CRLF1* compared to BMSC pellets transduced with empty AAV (Figure 4A). Contrary, reducing CRLF1 expression using siRNA specific for *CRLF1* (*CRLF1* siRNA) markedly reduced the mRNA levels of aggrecan, type II collagen, and Sox-9 in BMSC pellets cultured for 8 days in chondrogenic differentiation medium. mRNA levels of the hypertrophic markers, type X collagen and MMP-13, were also reduced in BMSC pellets transfected with CRLF1 siRNA compared to the mRNA levels of these markers in BMSC pellets transfected with control siRNA and cultured for 8 days in chondrogenic differentiation

medium (Figure 4B). These findings reveal that CRLF1 stimulates chondrogenic differentiation, while inhibiting hypertrophic differentiation.

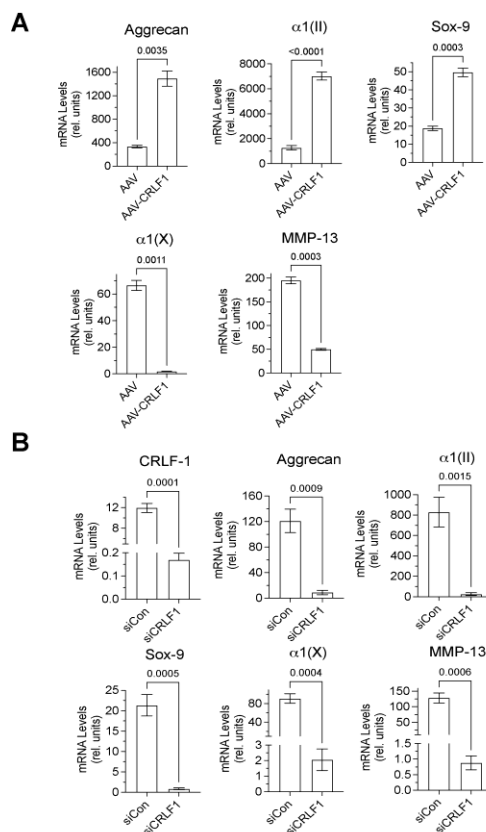


Figure 4. mRNA levels of chondrogenic markers in pellet cultures of BMSCs transduced with empty AAV or AAV containing CRLF1 A: mRNA levels of articular chondrocyte markers (Aggrecan, type II collagen $\alpha 1(II)$, Sox-9), hypertrophic differentiation markers (type X collagen $\alpha 1(X)$, MMP-13) at day 8 of BMSC pellets transduced with empty AAV (Empty AAV) or AAV containing CRLF1 (AAV-CRLF1) and cultured in chondrogenic differentiation medium for 8 days. B: mRNA levels of CRLF1, articular chondrocyte markers (Aggrecan, type II collagen $\alpha 1(II)$, Sox9), hypertrophic differentiation markers (type X collagen $\alpha 1(X)$, MMP-13) at day 8 of BMSC pellets transfected with control siRNA (siCon) or siRNA specific for CRLF1 (siCRLF1) and cultured in chondrogenic differentiation medium for 8 days. mRNA levels in A and B were determined by real-time PCR using SYBR Green and normalized to the level of 18S RNA. The mRNA levels are expressed relative to the levels of BMSC pellets transduced with empty AAV or control siRNA cultured for 1 day in chondrogenic differentiation medium, which was set as 1. Data were obtained from triplicate PCRs using RNA from 3 different cultures ($n = 3$), and are expressed as mean \pm SD. Statistical analysis between the two groups was carried out using Tukey's post hoc test; p values are indicated above the graphs.

3.3. CRLF1 Forms Homodimers When Overexpressed in BMSCs

CRLF1 mRNA levels in BMSCs transduced with AAV-CRLF1 were markedly increased compared to the levels in BMSCs transduced with empty AAV. Overexpression of CRLF1 did not increase the mRNA levels of CLC (Figure 5A). Immunoblot analysis using antibodies specific for CRLF1 of the culture medium revealed a markedly more intense band for CRLF1 in the medium from BMSCs transfected with AAV-CRLF1 compared to the intensity of the CRLF1 band in the medium from BMSCs transfected with empty AAV (Figure 5B). Under non-reducing conditions, a CRLF-1 immuno-positive band was identified with a molecular weight of ~ 110 kDa in the medium from BMSCs transfected with AAV-CRLF1 (Figure 5C). Upon reduction, we detected a 55 kDa CRLF1 band, which is consistent with monomeric CRLF1 (Figure 5C). The 110 kDa band in non-reducing gels was not detectable with antibodies specific for CLC confirming that the 110 kDa band represents

the homodimeric form of CRLF1 and not a heterodimeric CRLF1/CLC form. A 22 kDa band corresponding to the CLC monomeric form was detectable in the immunoblots of gels run under non-reducing and reducing conditions with antibodies specific for CLC (Figure 5C).

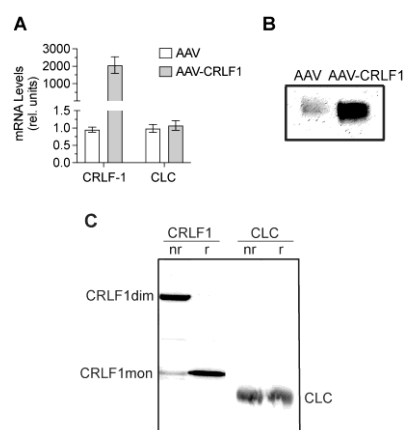


Figure 5. mRNA and protein levels of CRLF1 in human BMSCs after transduction with empty AAV or AAV containing *CRLF1*. **A:** mRNA levels of CRLF1 and CLC in BMSCs 4 days after transduction with empty AAV or AAV containing *CRLF1* (AAV-CRLF1). Levels of mRNA were determined by real-time PCR using SYBR Green and normalized to the level of 18S RNA. Data were obtained from triplicate PCRs using RNA from 3 different cultures ($n = 3$), and are expressed as mean \pm SD. Statistical analysis between the two groups was carried out using Tukey's post hoc test; p values are indicated above the graphs. **B:** Immunoblot analysis of conditioned medium collected from BMSCs transduced with empty AAV (AAV) or AAV-CRLF1 using antibodies specific for CRLF1. **C:** Immunoblot analysis of conditioned medium collected from BMSCs transduced with AAV-CRLF1 using antibodies specific for CRLF1 (CRLF1) or antibodies specific for CLC (CLC) of SDS gels that were run under non-reducing (nr) and reducing (r) conditions. CRLF1dim indicates the CRLF1 homodimeric form in the non-reducing gel, while CRLF1mon indicates the CRLF1 monomeric form in the reducing gel. CLC indicates the CLC monomeric form.

3.4. Effect of CRLF1 and CRLF1/CLC on Chondrocytes in an Inflammatory Environment

To determine how CRLF1 or the CRLF1/CLC complex affects chondrocytes in an inflammatory environment, we cultured human chondrocyte cell line TC28a2 in the presence of IL-1b and in the absence of presence of the CRLF1/CLC complex. For overexpression of CRLF1, TC28a2 cells were transfected with the expression vector pcDNA containing *CRLF1* followed by treatment with IL-1b for 24h. IL-1b treatment increased the mRNA levels of IL-6 and MMP-13. The CRLF1/CLC complex further increased the mRNA levels of IL-6 and MMP-13 in IL-1b-treated TC28a2 cells, whereas TC28a2 cells that overexpressed CRLF1 showed reduced mRNA levels of IL-6 and MMP-13 in the presence of IL-1b (Figure 6A). Treatment of cells with CRLF1/CLC heterodimeric complex resulted in the phosphorylation of STAT3, a primary effector of signaling by this complex. STAT3 signaling is considered one of the major catabolic signaling pathways in osteoarthritis [17]. In contrast, TC28a2 cells that overexpressed CRLF1 did not show an increased level of phosphorylated STAT3 (Figure 6B).

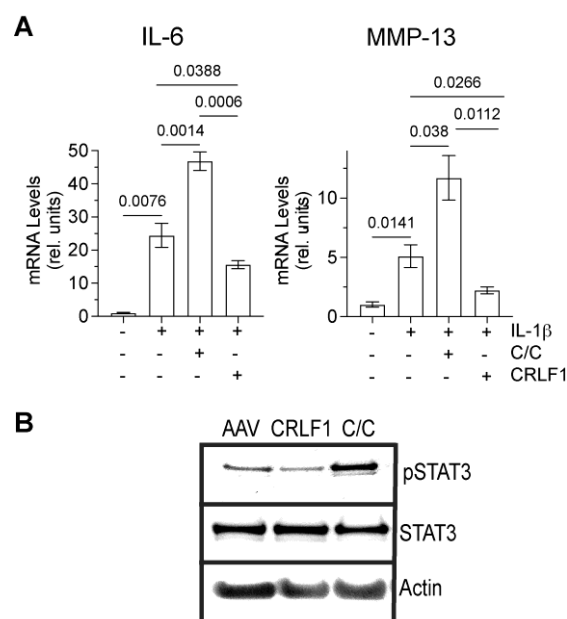


Figure 6. mRNA levels of catabolic markers and STAT3 signaling in IL-1b-treated TC28a2 cells overexpressing CRLF1 or in the presence of CRLF1/CLC complex. **A:** mRNA levels of catabolic markers IL-6 and MMP-13 in IL-1b-treated TC28a2 chondrocyte cell line overexpressing CRLF1 or in TC28a2 cells treated with IL-1b and the heterodimeric complex of CRLF1 and CLC (C/C). mRNA levels were determined by real-time PCR using SYBR Green and normalized to the level of 18S RNA. The mRNA levels are expressed relative to the levels of TC28a2 cells transduced with empty AAV, which was set as 1. Data were obtained from triplicate PCRs using RNA from 3 different cultures ($n = 3$), and are expressed as mean \pm SD. Statistical analysis between the two groups was carried out using Tukey's post hoc test; p values are indicated above the graphs. **B:** Phosphorylated (pSTAT3) and total STAT3 immunoblots of lysates from TC28a2 cells transduced with empty AAV (AAV), transduced with AAV containing CRLF1 (CRLF1), or treated with the heterodimeric CRLF1/CLC complex (C/C). Immunoblots for b-actin (Actin) were performed to demonstrate loading of equal protein concentration of each lysate.

4. Discussion

CRLF1, as well as the other IL-6 cytokines, can drive both regenerative and degenerative outcomes via selective and context/cell specific activation of various signaling modules within gp130 receptor in various tissues (3, 5). CRLF1 is expressed in bone and cartilage, and several studies have shown increased expression of CRLF1 in early-stage OA cartilage (3, 5-7, 16). However, the exact role of CRLF1 in cartilage homeostasis, regeneration and pathology is not known. In this study, we show that overexpression of CRLF1 enhanced chondrogenic differentiation of human BMSCs, while inhibition of CRLF1 expression inhibited chondrogenic differentiation. In addition, when CRLF1 was overexpressed in the chondrocyte cell line TC28a2, catabolic events stimulated by IL-1b were reduced. In contrast, when treated with the CRLF1/CLC heterodimeric complex, catabolic events were increased in IL-1b-treated TC28a2 cells. These findings suggest that CRLF1 uses different signaling pathways that have different effects on the phenotype and function of mesenchymal stem cells and chondrocytes.

Previous studies have shown that CRLF1 can form a homodimeric complex and heterodimeric complex with CLC, another member of the IL-6 cytokine family (3, 9). Our study shows that the overexpression of CRLF1 in human BMSCs (transduced with AAV containing *CRLF1*) resulted in the release of a homodimeric complex of CRLF1. More importantly, intra-articular injections of BMSCs overexpressing CRLF1 were more effective in improving the repair of an osteochondral defect in rabbit knee joints than intra-articular injections of BMSCs that do not overexpress CRLF1 (transduced with empty AAV). These findings suggest that the homodimeric form of CRLF1 is more efficient in

promoting osteochondral defect repair than the non homodimeric form of CRLF1. Our findings are in agreement with previous findings showing that only the homodimeric complex of CRLF1 is neuroprotective and protects neurons from oxidative stress (9).

The signaling of the heterodimeric complex of CRLF1 and CLC involves the use of a receptor subunit ciliary neurotrophic factor receptor (CNTFR) (3). The resulting complex then recruits the ubiquitously expressed receptor subunit gp130 and LIFR activating STAT3 signaling (4). In this study, we show that STAT3 signaling was activated when the chondrocytic cell line TC28a2 was treated with the heterodimeric CRLF1/CLC complex. When these cells, however, overexpressed CRLF1, STAT3 signaling was not activated. Our findings confirm previous findings showing that the homodimeric form of CRLF1 does not activate STAT3 signaling during neuroprotection from oxidative stress (9). Currently, no receptor has been identified, which the homodimeric CRLF1 complex binds. It is, however, also possible that the homodimeric complex of CRLF1 acts as a decoy receptor that neutralizes the heterodimeric CRLF1/CLC complex in the extracellular environment or inside the cell. Future studies need to address whether CRLF1 homodimers bind directly to the cell surface of MSCs and/or chondrocytes, which would indicate the presence of receptors that could potentially mediate signaling by the homodimeric CRLF1 complex.

Overexpression of CRLF1 in human BMSCs increased chondrogenic differentiation of these cells in the presence of TGFb1. TGFb-mediated Smad2 and 3 signaling has been shown to play a crucial role in chondrogenic differentiation and articular cartilage repair [18]. In addition, increased Smad2 and 3 signaling during chondrogenesis has been shown to inhibit hypertrophic and terminal differentiation of chondrocytes [18,19]. Our findings show an increased Smad2 and 3 activation, increased chondrogenesis and decreased hypertrophic differentiation of BMSCs overexpressing CRLF1 compared to BMSCs that do not overexpress CRF1. These findings suggest that CRLF1 may affect chondrogenesis via the regulation of TGFb/Smad signaling. Previous studies have shown that CRLF1 expression is upregulated by TGFb [6,20], suggesting a positive feedback loop during chondrogenic differentiation of BMSCs, in which increased amounts of CRLF1 further stimulate TGFb-mediated chondrogenic differentiation.

CRLF1 expression has been shown to be increased in osteoarthritic cartilage [4,6,7,21]. In addition, a previous study has shown that the CRLF1/CLC complex stimulates chondrocyte proliferation and suppressed the expression of aggrecan and type II collagen [6]. Our study reveals that a homodimeric complex of CRLF1 stimulated chondrogenic differentiation of human BMSCs and reduced catabolic events in IL-1b-treated chondrocytes, while a heterodimeric complex of CRLF1 and CLC stimulated catabolic events in chondrocytes. Our findings contradict findings from a previous study showing that CRLF1 causes apoptosis in murine BMSCs and inhibits the chondrogenic differentiation of these cells [22]. The study by Xu et al. [22], however, did not determine whether CRLF1 constituted into a homodimeric form or heterodimeric form with CLC in murine BMSC cultures. Therefore, it is plausible to suggest that a heterodimeric complex of CRLF1 and CLC may lead to apoptosis of MSCs and inhibition of their chondrogenic differentiation, while a homodimeric CRLF1 complex leads to the stimulation of chondrogenic differentiation of BMSCs. As shown in other [9] and our studies, the homodimeric CRLF1 complex results in different signaling than the heterodimeric CRLF1 and CLC complex ultimately resulting in a different outcome on cell phenotype.

Limitations of our study include the use of a small animal model. The osteochondral defect model in rabbits is well established and validated [12–14]. Rabbits, however, have faster skeletal change and bone turnover than other species and humans. Furthermore, rabbits have different gait patterns from those in humans. In addition, even though, none of the rabbits in our study experienced any adverse events to the intra-articular injection of human BMSCs that were transduced with AAV, we did not perform detailed pharmacological and toxicological analyses. Finally, we did not determine whether the injected BMSCs directly contributed to the repair of the osteochondral defect or indirectly via the release of soluble factors, including CRLF1, and extracellular vesicles. A final limitation of this study is lack of considering sex as a potential variable. In the current study we only

used male rabbits. Before translating our findings into clinical studies, we need to address all the mentioned limitations of the current study.

5. Conclusions

Our study shows that overexpression of CRLF1 in BMSCs greatly enhances their effectiveness in improving the repair of osteochondral defects in rabbits compared to BMSCs that do not overexpress CRLF1. Specifically, our findings suggest that the homodimeric form of CRLF1 released by BMSCs overexpressing CRLF1 leads to the stimulation of chondrogenic differentiation of precursor cells and to an inhibition of catabolic events in articular chondrocytes. Both events are crucial for the improvement of the repair of an osteochondral defect. Therefore, our findings suggest that the homodimeric form of CRLF1 may provide a novel therapeutic strategy to improve the repair of osteochondral defects.

Supplementary Materials: The following supporting information can be downloaded at the website of this paper posted on Preprints.org, Table S1: Eight histological and immunohistological parameters selected for quantification of Cartilage Repair as per International Cartilage Repair Society II Scoring System with Slight Modifications.

Author Contributions: Conceptualization, K.A.C., A.J.C. and T.K.; methodology, A.J.C, J.F.D, T.K. and F.Z.; validation, J.F.D, and F.Z.; formal analysis, T.K., F.Z.; investigation, A.J.C., J.F.D, Y.J.L and F.Z.; resources, T.K.; data curation, T.K., H.J.L. and F.Z.; writing—original draft preparation, T.K.; writing—review and editing, K.A.C., J.F.D., T.K. and F.Z.; supervision, K.A.C. and T.K.; project administration, A.J.C. and T.K.; funding acquisition, A.J.C. and T.K. All authors have read and agreed to the published version of the manuscript.

Funding: This research was funded by National Institute of Arthritis and Musculoskeletal and Skin Diseases, R21AR075132 to T.K. and by the Orthopaedic Research and Education Foundation (OREF), Resident Research Grant 109977 to A.J.C.

Data Availability Statement: The data presented in this study are available on reasonable request from the corresponding author.

Conflicts of Interest: The authors declare no conflicts of interest.

References

1. Farr, J.; Cole, B.; Dhawan, A.; Kercher, J.; Sherman, S. Clinical cartilage restoration: evolution and overview. *Clin Orthop Relat Res* **2011**, *469*, 2696–2705.
2. Makris, E.A.; Gomoll, A.H.; Malizos, K.N.; Hu, J.C.; Athanasiou, K.A. Repair and tissue engineering techniques for articular cartilage. *Nat Rev Rheumatol* **2015**, *11*, 21–34.
3. Sims, N.A. Cardiotrophin-like cytokine factor 1 (CLCF1) and neuropoietin (NP) signalling and their roles in development, adulthood, cancer and degenerative disorders. *Cytokine Growth Factor Rev* **2015**, *26*, 517–522.
4. Crisponi, L.; Buers, I.; Rutsch, F. CRLF1 and CLCF1 in development, health and disease. *Int J Mol Sci* **2022**, *23*.
5. Silver, J.S.; Hunter, C.A. gp130 at the nexus of inflammation, autoimmunity, and cancer. *J Leukoc Biol* **2010**, *88*, 1145–1156.
6. Tsuritani, K.; Takeda, J.; Sakagami, J.; Ishii, A.; Eriksson, T.; Hara, T.; Ishibashi, H.; Koshihara, Y.; Yamada, K.; Yoneda, Y. Cytokine receptor-like factor 1 is highly expressed in damaged human knee osteoarthritic cartilage and involved in osteoarthritis downstream of TGF-beta. *Calcif Tissue Int* **2010**, *86*, 47–57.
7. Bateman, J.F.; Rowley, L.; Belluoccio, D.; Chan, B.; Bell, K.; Fosang, A.J.; Little, C.B. Transcriptomics of wild-type mice and mice lacking ADAMTS-5 activity identifies genes involved in osteoarthritis initiation and cartilage destruction. *Arthritis Rheum* **2013**, *65*, 1547–1560.
8. Sato, T.; Konomi, K.; Yamasaki, S.; Aratani, S.; Tsuchimochi, K.; Yokouchi, M.; Masuko-Hongo, K.; Yagishita, N.; Nakamura, H.; Komiyama, S.; et al. Comparative analysis of gene expression profiles in intact and damaged regions of human osteoarthritic cartilage. *Arthritis Rheum* **2006**, *54*, 808–817.
9. Looyenga, B.D.; Resau, J.; MacKeigan, J.P. Cytokine receptor-like factor 1 (CRLF1) protects against 6-hydroxydopamine toxicity independent of the gp130/JAK signaling pathway. *PLoS One* **2013**, *8*, e66548.
10. Minashima, T.; Kirsch, T. Annexin A6 regulates catabolic events in articular chondrocytes via the modulation of NF-kappaB and Wnt/ss-catenin signaling. *PLoS One* **2018**, *13*, e0197690.
11. Wang, W.; Kirsch, T. Retinoic acid stimulates annexin-mediated growth plate chondrocyte mineralization. *J Cell Biol* **2002 Jun** *10*, *157*, 1061-1069.

12. Danna, N.R.; Beutel, B.G.; Ramme, A.J.; Kirsch, T.; Kennedy, O.D.; Strauss, E. The effect of growth hormone on chondral defect repair. *Cartilage* **2018**, *9*, 63–70.
13. Strauss, E.; Schachter, A.; Frenkel, S.; Rosen, J. The efficacy of intra-articular hyaluronan injection after the microfracture technique for the treatment of articular cartilage lesions. *Am J Sports Med* **2009**, *37*, 720–726.
14. Jiang, G.; Li, S.; Yu, K.; He, B.; Hong, J.; Xu, T.; Meng, J.; Ye, C.; Chen, Y.; Shi, Z.; et al. A 3D-printed PRP-GelMA hydrogel promotes osteochondral regeneration through M2 macrophage polarization in a rabbit model. *Acta Biomater* **2021**, *128*, 150–162.
15. Smith, G.D.; Taylor, J.; Almqvist, K.F.; Erggelet, C.; Knutsen, G.; Garcia Portabella, M.; Smith, T.; Richardson, J.B. Arthroscopic assessment of cartilage repair: a validation study of 2 scoring systems. *Arthroscopy* **2005**, *21*, 1462–1467.
16. Mainil-Varlet, P.; Aigner, T.; Brittberg, M.; Bullough, P.; Hollander, A.; Hunziker, E.; Kandel, R.; Nehrer, S.; Pritzker, K.; Roberts, S.; et al. Histological assessment of cartilage repair: a report by the Histology Endpoint Committee of the International Cartilage Repair Society (ICRS). *J Bone Joint Surg Am* **2003**, *85-A Suppl 2*, 45–57.
17. Wiegertjes, R.; van de Loo, F.A.J.; Blaney Davidson, E.N. A roadmap to target interleukin-6 in osteoarthritis. *Rheumatology (Oxford)* **2020**, *59*, 2681–2694.
18. Ying, J.; Wang, P.; Zhang, S.; Xu, T.; Zhang, L.; Dong, R.; Xu, S.; Tong, P.; Wu, C.; Jin, H. Transforming growth factor-beta1 promotes articular cartilage repair through canonical Smad and Hippo pathways in bone mesenchymal stem cells. *Life Sci* **2018**, *192*, 84–90.
19. Zhang, T.; Wen, F.; Wu, Y.; Goh, G.S.; Ge, Z.; Tan, L.P.; Hui, J.H.; Yang, Z. Cross-talk between TGF-beta/SMAD and integrin signaling pathways in regulating hypertrophy of mesenchymal stem cell chondrogenesis under deferral dynamic compression. *Biomaterials* **2015**, *38*, 72–85.
20. Luo, S.; Yang, Z.; Chen, R.; You, D.; Teng, F.; Yuan, Y.; Liu, W.; Li, J.; Zhang, H. Cytokine receptor-like factor 1 (CRLF1) promotes cardiac fibrosis via ERK1/2 signaling pathway. *J Zhejiang Univ Sci B* **2023**, *24*, 682–697.
21. Tew, S.R.; Clegg, P.D.; Brew, C.J.; Redmond, C.M.; Hardingham, T.E. SOX9 transduction of a human chondrocytic cell line identifies novel genes regulated in primary human chondrocytes and in osteoarthritis. *Arthritis Res Ther* **2007**, *9*, R107.
22. Xu, H.; Ding, C.; Guo, C.; Xiang, S.; Wang, Y.; Luo, B.; Xiang, H. Suppression of CRLF1 promotes the chondrogenic differentiation of bone marrow-derived mesenchymal stem and protects cartilage tissue from damage in osteoarthritis via activation of miR-320. *Mol Med* **2021**, *27*, 116.

Disclaimer/Publisher's Note: The statements, opinions and data contained in all publications are solely those of the individual author(s) and contributor(s) and not of MDPI and/or the editor(s). MDPI and/or the editor(s) disclaim responsibility for any injury to people or property resulting from any ideas, methods, instructions or products referred to in the content.